Vibrational quenching at ultralow energies: Calculations of the $Li_2(^1\Sigma_g^+; \nu \gg 0)$+He superelastic scattering cross sections

Enrico Bodo and Franco A. Gianturco*
Department of Chemistry, University of Rome La Sapienza, Piazzale A. Moro 5, 00185 Rome, Italy

Ersin Yurtsever
Department of Chemistry, Koç University, Istanbul, Turkey
(Received 27 February 2006; published 31 May 2006)

Accurate quantum calculations have been carried out at ultralow energies (from 10^{-2} to 10^{-6} cm^{-1}) for the vibrational deexcitation of $Li_2(^1\Sigma_g^+)$ by collisions with He, starting from a broad range of initial highly excited vibrational levels. The results indicate the clear dominance of a few transitions with the smallest $\Delta\nu$ changes and show the overall deexcitation cross sections to markedly depend on the initial vibrational state of the molecule, in line with earlier results on H_2+He [Balakrishan *et al.* Phys. Rev. Lett. **80**, 3224 (1998)] vibrational quenching. A connection is made with very recent measurements on the vibrational quenching of ultracold Cs_2 molecules in optical traps that were instead found to behave in a very different manner. Numerical experiments on the present system as well as on the H_3 reaction strongly suggest a possible explanation for such differences.

DOI: 10.1103/PhysRevA.73.052715 PACS number(s): 34.30.+h, 34.50.−s

I. INTRODUCTION

As the physics of low temperatures in magnetic and optical traps has moved beyond the analysis of dilute gases containing only atoms, a new area of interest in many-body, chemical behavior at ultralow temperatures is clearly beginning to emerge [1–4]. Ultralow-temperature measurements of the cross section of collisional processes like vibrational or rotational quenching or even exothermic chemical reactions are, however, extremely difficult to obtain because the storage and the cooling of molecules is indeed more complicated than that of atomic species. Laser cooling techniques, in fact, cannot be easily extended to molecules because of their complex multilevel internal structures [1]. One way in which one can create ultracold molecules is by first producing cold atoms and then forming excited molecules by photoassociation processes. The latter species are fairly short lived as they are vibrationally excited and tend to release internal energy via vibrational deexcitation unless a stabilization procedure is introduced in order to bring the molecule to its ground state [5]. Another method for forming cold molecules out of cold atoms is based on the possibility of inducing a resonant atomic collision when the position of a suitable Feshbach resonance is tuned through the use of an additional magnetic field in the trap [6–9]. In this case the molecules created from bosonic atoms are unstable with respect to vibrational quenching while those obtained from fermionic atoms remain stable for longer times; this effect being probably due to a phenomenon similar to Pauli blocking in fermion-fermion collisions [10–12]. On the other hand, experiments where polar molecules are cooled through the use of He as a buffer gas [13,14] offer the opportunity of measuring vibrational [15] and rotational quenching rates with which theoretical data may be compared. Furthermore, the stability of rotationally hot molecules in a cold buffer gas has been explored theoretically in the case of atom-molecule collisions [16] and the importance of resonant energy transfer mechanisms at ultralow energies has been confirmed.

Among the various sources of instability that plague the experiments dealing with these ensemble of ultracold diatomic molecules (formed through either photoassociation or directly via a Feshbach resonance) collisional deexcitation of vibrationally excited states is one of the most effective in limiting the lifetime of the molecular ensemble. However, the dynamics of vibrational quenching from highly excited states is still poorly understood and only two calculations, as far as we know, have been published thus far: one on the H_2+H system [17,18] and another for the H_2+He system [19]. On the other hand, much more work has been done for systems where the target molecule is only weakly excited to its lower levels: see, for example, Refs. [15,20–22]. Additionally, when chemical reactions can take place during the atom-molecule collision as is the case for typical A_3 systems made of alkali-metal atoms, the calculation becomes much more complex and therefore only exploratory computations have been performed for Li_3 [23] and K_3 [24] so far.

In two recent experiments, Weidemuller and co-workers [25] and Pillet and co-workers [26] have independently measured the rate of vibrational deexcitation for Cs_2 from highly vibrational states in collision with Cs atoms and found that the rates did not depend much upon the initial vibrational state of the molecule. For example, in Ref. [25] the inelastic rate coefficients for both $Cs_2(\nu=32-47)$ and $Cs_2(\nu=4-6)$ are very near to 1×10^{-10} cm^3 s^{-1}. On the other hand a coefficient of about 2.5×10^{-11} cm^3 s^{-1} has been reported in Ref. [26] for a similar transition.

Stimulated by such recent experiments, this paper presents an analysis of vibrational deexcitation processes for the lithium dimer in its singlet state $Li_2(^1\Sigma_g^+)$, which is presumed to have been formed in one of its highly excited vibrational

*Corresponding author. FAX: +39-06-49913305. Email address: fa.gianturco@caspur.it

levels (it supports a total of 42 vibrational levels for the $j=0$ rotational state) and which is then made to collide with ^{4}He at ultralow energies such as those that can exist in an optical trap. The choice of this system is simply motivated by the fact that it has the computational advantage of not including any reactive channel (LiHe is not bound) and therefore we can correctly describe the collision process using the somewhat simpler dynamics of inelastic scattering only. This situation has allowed us to include a number of rovibrational states in our computation which would have been nearly impossible to include in a reactive system like Li_3.

In the next section we report the relevant features of the potential energy surface we have employed. In Sec. III we report our results for the vibrational deexcitation and in Sec. IV a numerical experiment that might help us to understand the discrepancy between the theoretical predictions and the experimental results.

II. INTERACTION AND QUANTUM DYNAMICS

It is already well known that the magnitude of the collisional quenching is largely determined by the intermolecular forces which act between the cold atoms and the molecules. Since quantum-mechanical effects play a dominant role at low energies, the ensuing scattering attributes become particularly sensitive to fine details in the intermolecular potentials. In the present instance of the collisional relaxation of a vibrationally excited diatomic target the internal energy of the molecule in the entrance channel (E_i) is larger than that in the exit channel (E_f). Hence, at the threshold of the entrance channel the exit one is already open and the internal energy difference ΔE_{if} appears entirely as kinetic energy in the outgoing channel. The corresponding exothermic cooling process is therefore the result of superelastic scattering: the corresponding inelastic cross section tends to infinity in the limit of zero kinetic energy of the incoming atom as established by Wigner's threshold law [27].

A. The potential energy surface

In the case of the present van der Waals system, the vibrational coupling potential has been modeled years ago [28] using a set of parameters which were adjusted to reproduce experimental data from molecular beams at much higher energies (80 meV) than those we intend to study here. Those early results suggested that anisotropic effects were coupled to vibrational effects while translational and vibrational motions were only weakly coupled. In a more recent study of the interaction forces in the case of a Li_2 target treated as a rigid rotor (RR) [29], our *ab initio* generation of the potential anisotropy and range of action showed this system to be coupling the target molecule very weakly with the He atom and to provide bound states only in the case of at least three helium partners with the $Li_2(^1\Sigma_g^+)$ target. Subsequently, a further study of the same RR potential introduced a more accurate description of two-body (2B) forces to be added to the three-body (3B) forces of [29] in order to obtain a better description of the overall potential [30]. It was found there that the modified potential energy surface (PES) showed a stronger orientational anisotropy and increased its well depth for both the C_{2v} and $C_{\infty v}$ orientations: it also supported a bound state for the Li_2(He) and $Li_2(He)_2$ complexes [30].

We have once more extended the above studies to include the explicit dependence of the interaction on the internal molecular coordinate, thereby producing the interaction potential over a range of r values for the Li_2 bond from 2.1 to 15.0 Å for a total of 3640 additional points. The Jacobi angles used were $\vartheta=0°$, 30°, 60°, and 90° and the entire set of *ab initio* energies was produced via quadratic configuration interaction with singles, doubles, and noniterative corrections to the triples [QCISD(T)] with a cc-pVQZ basis set. Some of the calculations were repeated using the coupled-cluster method [CCSD(T)] with the same basis set and the two sets of values were found to coincide within 10^{-6}%.

The resulting PES was then fitted analytically with the following method. We generated the nonseparable three-body interaction using the expression

$$V_{3B}(r_1,r_2,r_3) = V_{Li_2He}(r_1,r_2,r_3) - V_{Li_2}(r_1) - V_{LiHe}(r_2) - V_{LiHe}(r_3) \quad (1)$$

which was then fitted using the Aguado-Paniagua type of expansion [31]. Our interaction potential is then constructed out of the sum of this three-body potential plus two accurate Li–He diatomic contributions that we have taken from Ref. [32].

In order to perform scattering calculations the rovibrational wave functions of the isolated Li_2 molecule are needed. We have used the RKR potential available in the literature [33] with the long-range part of the potential obtained from Ref. [34]. This finally "fused" form of the PES of Li_2 (for $J=0$) supports 42 vibrational levels in close agreement with the ones reported in the above papers. Just to give a pictorial feeling of the spatial extensions over the vibrational coordinate for the various levels involved, we report in Fig. 1 the lowest two bound-state wave functions (WFs) ($\nu=0$ and 1) and four of the densities associated with some of the excited levels ($\nu=18$, 19, 29, and 30); the radial changes as ν increases are clearly quite marked.

The quantum coupling equations for the dynamics, as we shall discuss in the next section, require knowledge of the individual coupling matrix elements of the full potential over the asymptotic (diabatic) vibrational target WF's

$$V_{\nu\nu'}(R,\vartheta) = \langle \chi_\nu(r)|V(r,R,\vartheta)|\chi_{\nu'}(r)\rangle \quad (2)$$

where the χ_i's are the numerical solutions of the target vibrational equation using the selected asymptotic potential.

One important quantity to know is the strength and spatial extension of such coupling potential terms since they are responsible for the final flux distributions into the available molecular channels after the superelastic collision. We report in Fig. 2 the radial dependence, for two specific orientations, of a few diagonal matrix elements obtained from the numerical integration of Eq. (1). The panel on the left reports the data for $\vartheta=90°$, while the one on the right refers to the collinear approach ($\vartheta=0°$). One clearly sees that the potential strength decreases as the molecule is initially vibra-

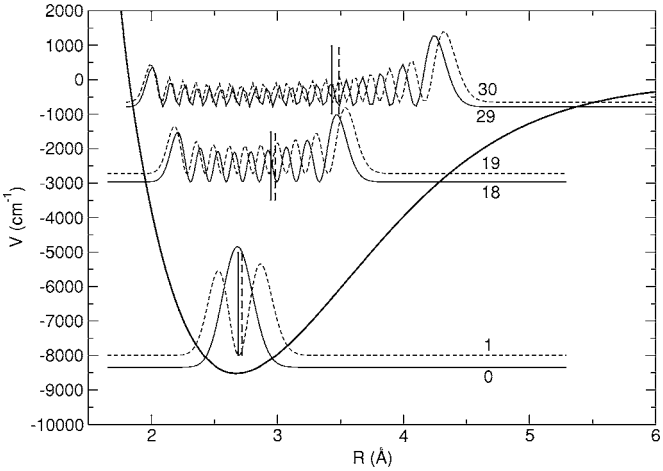

FIG. 1. Computed vibrational WFs $|\Psi_\nu|^2$ for the lowest two states ($\nu=0,1$) and for representative excited states ($\nu=18$, 19, 29, and 30). Energies in cm^{-1}, distances in Å. Vertical bars identify graphically the average internuclear distances $\langle r\rangle$ for each vibrational state.

tionally more excited, a feature related to the reduced potential coupling strength for the spatially more extended initial target states. This will affect the asymptotic values of the elastic cross sections which, according to the Wigner threshold law [27], will tend to a constant value at vanishing collision energies, as we will further discuss in the following section.

The vibrational cooling process between neighboring levels, on the other hand, is controlled by the size and strength of the off-diagonal matrix elements differing by one or more quantum number: the computed results from Fig. 3 show the radial and angular behavior of such coupling potential terms for a range of representative levels as already discussed for Fig. 2. The energy scale of the coupling strength is now obviously much smaller and we see that, on the left panel, the various contributions remain of the same order of magnitude as we go up the vibrational ladder: neighboring levels are therefore coupled by similar matrix elements, no matter

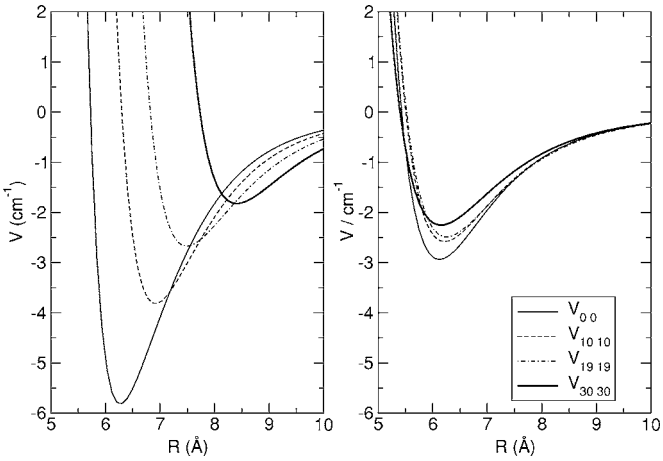

FIG. 2. Computed coupling matrix elements (diagonal terms) from Eq. (1) and for a representative set of vibrational target states. Left panel: for $\vartheta=90°$; right panel: for $\vartheta=0°$.

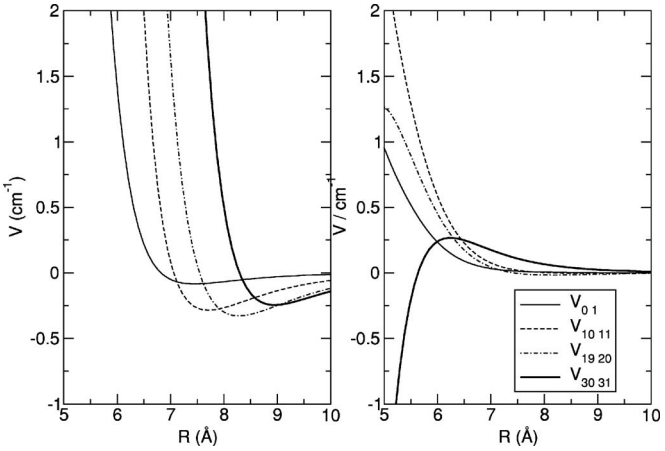

FIG. 3. Computed off-diagonal vibrational coupling potential terms for the same orientation of Fig. 2.

where they are located along the excitation sequence at least for ν values still far from dissociation.

B. Quantum dynamics and the threshold laws

When solving the time-independent quantum scattering equations we first expand the total wave function in terms of products of vibrational and rotational states of the diatomic molecule

$$\Psi_{tot}(r,R,\vartheta)=\frac{1}{R}\sum_{J,\nu,j,l,m_l} f_{\nu j}^{Jl}(R)\chi_\nu^j(\mathbf{r})Y_l^{m_l}(\hat{\mathbf{R}}\cdot\hat{\mathbf{r}}). \tag{3}$$

The vibrational wave functions and the target rovibrational levels $\varepsilon_i=\varepsilon_{\nu j}$ are obtained by solving the Schrödinger equation for the diatom using the potential described previously.

The corresponding coupled-channel equations in the space-fixed (SF) reference frame are then given by

$$\left\{\frac{d^2}{dR^2}+\mathbf{k}^2-\mathbf{V}-\frac{\ell^2}{R^2}\right\}\mathbf{F}^J=0 \tag{4}$$

where, as usual, $[\mathbf{k}^2]_{ij}=\delta_{ij}2\mu[E-\varepsilon_i]$ is the diagonal matrix for the asymptotic (squared) wave vectors, the coupling matrix $\mathbf{V}=2\mu\mathbf{U}$ contains the full potential terms of Eq. (1), and ℓ^2 is the matrix representation of the square of the relative orbital angular momentum: $[\ell^2]_{ij}=\delta_{ij}\ell_i(\ell_i+1)$. The matrix $\mathbf{F}^J$ holds the radial solutions for each choice of the total angular momentum $\mathbf{J}$, the dynamical constant of the motion for the present system.

In the asymptotic region the solution matrix can be written as

$$\mathbf{\Psi}(R)=\mathbf{J}(R)-\mathbf{N}(R)\cdot\mathbf{K} \tag{5}$$

from which we obtain $\mathbf{K}$ and then $\mathbf{S}$ from the transformation $\mathbf{S}=(1+i\mathbf{K})^{-1}\cdot(1-i\mathbf{K})$ where $\mathbf{J}(R)$ and $\mathbf{N}(R)$ are diagonal matrices contain Riccati-Bessel and Riccati-Newmann functions. The corresponding state-to-state superelastic cross sections will be given by

$$\sigma_{\nu j\to\nu' j'}(E_i)=\frac{\pi}{(2j+1)k_{\nu j}^2}\sum_J(2J+1)\sum_{l,l'}|\delta_{l\nu j,l'\nu' j'}-S_{\nu j,\nu' j'}^{ll'}|^2. \quad (6)$$

The corresponding expansion of the elastic matrix element in powers of k allows one to write

$$S_{\nu j,\nu j}\simeq 1+2i\delta_{\nu j}(k)=1-2ik(\alpha_{\nu j}-i\beta_{\nu j})=1-2ika_{\nu j} \quad (7)$$

which allows us to obtain the real ($\alpha_{\nu j}$) and imaginary ($\beta_{\nu j}$) parts of the scattering length $a_{\nu j}$. The corresponding elastic and inelastic parts of the total scattering cross sections, in the same limit of $k\to 0$, are given by

$$\sigma_{\nu j}^{el}=4\pi|a_{\nu j}|^2,\quad \sigma_{\nu j}^{inel}=\frac{4\pi\beta_{\nu j}}{k}. \quad (8)$$

III. PRESENT RESULTS

The calculations have been done only for total angular momentum $J=0$ and for different initial vibrational states of the molecule, the latter being initially in the rotational $j=0$ state, and we have included in the basis set all the 42 vibrational states of the isolated molecule. We have also included up to $j_{max}=48$ for the open vibrational channels and up to $j_{max}=2$ for the closed vibrational ones. Such choices allowed us to obtain computed cross sections converged within 1%. In the whole treatment the rotational wave functions were considered as independent of the vibrational components and we further neglected the coupling with the continuum for the highly vibrationally excited target states which would be likely to become increasingly more important as we go above the $\nu=30$ vibrational quantum number. Even considering the above simplifications, our final basis sets grew to include up to 800 channels.

Ultralow and low energies between 10^{-6} and 1 cm^{-1} have been explored for specific initial vibrational states, while for others we have only performed calculations at the lowest energy, i.e., 1×10^{-6} cm^{-1}. The results reported in Fig. 4 show, in the left panel, the asymptotic behavior of the elastic cross section from the initial levels $\nu=30,25,20,15,10$, while the right-hand panel shows the $\Delta\nu=1$ inelastic cross section from the same initial states. It is clear in both cases that the Wigner regime is essentially achieved at around 10^{-2} cm^{-1} and down to the asymptotic limit. The elastic cross section is seen to be only weakly dependent on the initial ν while the inelastic ones show instead a much more marked variation with ν even if not as pronounced as the one that has been found in the earlier calculations of Refs. [17,19] for the H_2 molecule.

To try to shed more light on the elementary mechanisms that may be at play for this system, we report in Fig. 5 the cascading of the quenching processes, computed at the asymptotic energy of 10^{-6} cm^{-1}, from $\nu=30$, 20, and 15 as a function of the final ν' values. The results shown in the left panel of Fig. 5 clearly indicate, on a logarithmic scale, the dramatic reduction in size of the quenching cross sections as the quantum "jump" goes beyond $\Delta\nu=3$: a unit increase in $\Delta\nu$ roughly corresponds to at least a drop by one order of magnitude in the cross section. The rotational distributions within the final vibrational state are shown on the two panels on the right-hand side of Fig. 5. The top right panel reports the final-rotational-state distributions for the $\Delta\nu=1$ and 2 processes from the $\nu=30$ initial level: one clearly detects there the preferential population of the $j'=4$, 6, 8, and 10 final rotational levels. The potential anisotropy is therefore effective in producing vibrationally colder molecules which can, however, still be rotationally "hot" with respect to their initial j state. A similar mechanism is also at work for producing the results shown in the lower right panel of Fig. 5 where we present the final rotational distributions associated with $\Delta\nu=3$ and 10. During the vibrational quenching process, while the internal vibrational energy content decreases, sizable internal rotational energy could still be present in the molecules.

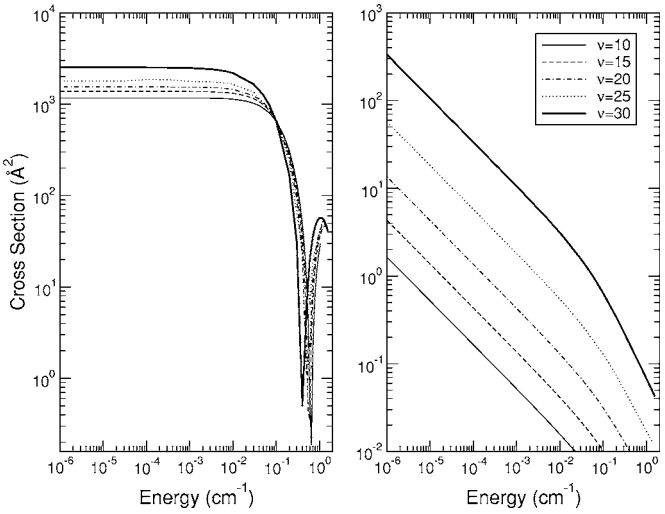

FIG. 4. Computed elastic (left) and inelastic (right) cross sections (in units of Å^2) as a function of collision energy values. See text for details.

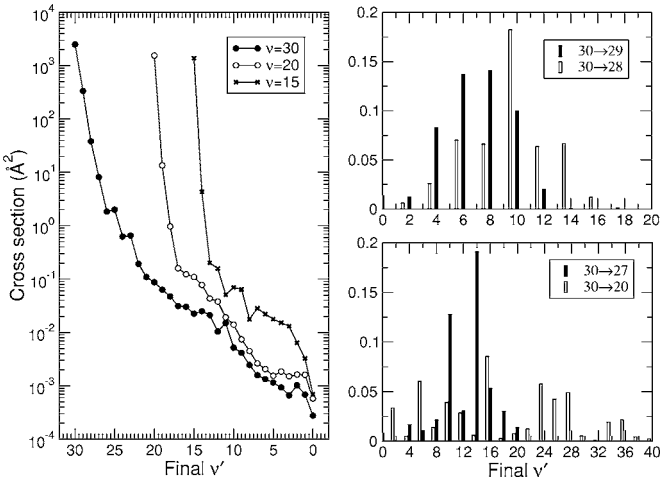

FIG. 5. Computed quenching cross sections from different initial ν values as functions of the final level ν' (left panel). The collision energy is 10^{-6} cm^{-1}. The right panels report the final, renormalized rotational distributions after the indicated vibrational transitions.

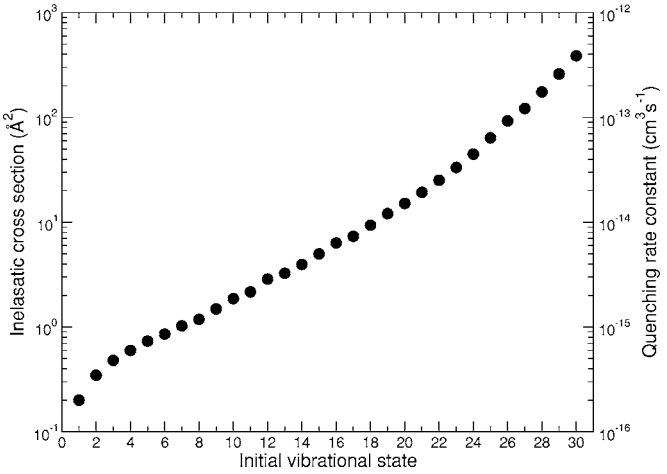

FIG. 6. Computed total quenching cross sections as a function of the initial state. The scale on the right measures the corresponding $T=0$ rate coefficient.

A further, global view of the processes we are considering in the present study is provided by the results shown by Fig. 6 where for each initial vibrational state we report both the total inelastic cross section (scale on the left) and the limiting value of the corresponding rate constant (scale on the right). We see that also for the present system the dependence upon the initial ν value is rather marked, although not as strong as that found in the $H+H_2$ system [17]. It is interesting to note, however, that our results are comparable to what had been previously found for H_2+He [19], another weakly interacting system.

IV. VIBRATIONAL LEVEL CONGESTION: A NUMERICAL EXPERIMENT

In the model calculations on $H+H_2$ [17], the authors showed that the relaxation of vibrationally excited H_2 in collision with H atoms, when the atom exchange process is neglected, provided rate constants values from all the vibrational levels of H_2 that varied by seven orders of magnitude between $\nu=0$ and 12. Also for the H_2+He inelastic process [19] the rate costants keep showing a similar range of variation over the range of initial vibrational levels of H_2. The calculations reported in the previous section have confirmed once more this behavior also in the Li_2+He system. On the other hand, the recent experiments on highly reactive and much heavier systems like Cs_2+Cs [25,26] estimated the inelastic rates to be largely independent of the initial vibrational state of the molecular partner and to remain between 10^{-10} and 10^{-11} cm^{-1}. In order to see the possible role played by the density of states (given the much large number of vibrational levels supported by the triplet ground state of Cs_2) we have repeated the calculations for the nonreactive collision in Li_2-He and in the reactive collision in H_2-H increasing the density of states in the diatomic molecules by arbitrarily increasing the masses of the Li and H atoms, respectively. In order to keep the calculation manageable we have included only the $j=0$ state for each vibrational level of the molecules considered: we shall call this scheme the rotationless approximation. Figure 7 reports our results for the reactive collision H_2+H obtained with the method and code of Ref. [35] and the PES from Refs. [36–38]. The panel on the left shows the total quenching cross section (calculated at 1×10^{-6} eV within the rotationless approximation) as the reduced mass is increased by only 50% with respect to its exact value. One clearly sees that only minimal changes are observed and the range of the relevant cross sections remains over seven order of magnitude. On the other hand, the panel on the right shows the same cross sections when the H mass is changed by one order of magnitude or more. One sees a very strong damping of the cross-section increase: it now remains around 10^2-10^3 Å^2 although still showing marked oscillations. The results of Fig. 8 report the exact and rotationless inelastic total quenching cross sections in the Li_2-He system obtained as in Fig. 6. The panel on the left shows the relatively small modifications due to the use of the rotationless approximation as in [19] instead of an exact procedure. The results of the panel on the right, on the other

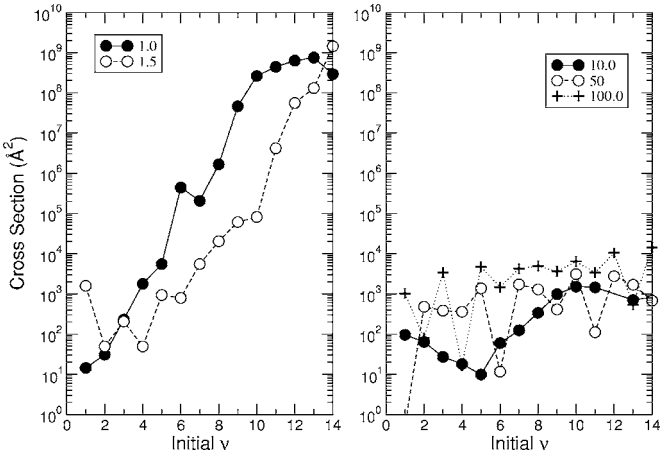

FIG. 7. Computed total reactive cross sections as a function of the initial vibrational state for H_2+H. Left panel, exact results and a small mass increase; right panel, large mass increase.

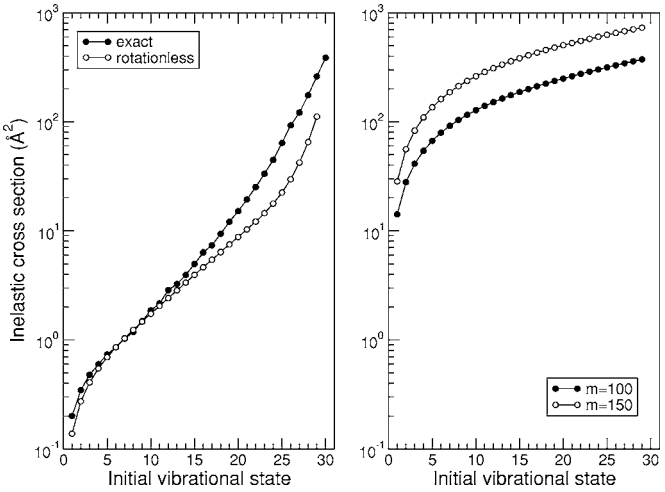

FIG. 8. Computed total quenching cross sections as a function of the initial vibrational state for Li_2+He. Left panel, exact and rotationless approximation; right panel, large mass increase.

hand, report the same inelastic cross sections when the diatomic mass is varied up to several sizes larger than the correct one. The calculations clearly indicate a flattening of the cross section's dependence on the initial vibrational level: we are now in a regime of "level congestion" which is more similar to that existing in Cs_2 ($\omega_e \sim 20$ cm^{-1} for triplet Cs_2 and is ~ 100 cm^{-1} for the heaviest Li_2). Therefore in spite of the differences in the interaction potentials and of the lack of reactive channels in the Li_2+He system, one clearly observes the much weaker dependence of the cross section with respect to the initial vibrational level. This is indeed what seems to have been observed in the mentioned experiments [25,26] and the present findings strongly suggest that such behavior could be partly determined by the much higher density of states in the heavier systems.

V. PRESENT CONCLUSIONS

In conclusion, we have carried out *ab initio* quantum computations for the vibrational deexcitation (quenching) cross sections of $Li_2(^1\Sigma_g^+, \nu)$ in collision with ^{4}He at ultralow energies. The scope of the study was to help our understanding of the collisional quenching processes seen to occur in ultracold traps used in recent experiments [25,26] where heavier alkali-metal systems were involved and where also chemical reactions were possible. We have employed an accurate potential energy surface recently obtained by us [30] which explicitly includes the dependence on the vibrational coordinate. The calculations have treated the dynamics using the coupled-channel expansion and have examined the relative size of the quenching cross sections as the initial target level is varied within a range of excited states, which went up to ν=30 in order to maintain an acceptable level of accuracy in the results as we did not include in the present quantum dynamics further coupling with the continuum states of the molecular target, a feature that becomes increasingly more necessary as one approaches levels close to dissociation. The present results indicate that the quenching cross sections for a light molecular partner have indeed a marked dependence on the initial vibrational quantum state of the target, a result which confirms the earlier findings on other van der Waals systems like H_2+He [19], where the same range of variation of the rate coefficients as ν varies was found to occur, and H_2+H [17], where an even broader range of variation was found.

In order to better understand, at the molecular level, the possible causes for the discrepancy found between the calculations (both ours and earlier ones) and the experiments on Cs_2-Cs we decided to carry out two distinct numerical experiments on both a reactive situation (H_2+H) and a nonreactive system (Li_2+He). Increasing the density of states of the asymptotic diatoms in the above systems leads to a weaker dependence of the deexcitation cross sections upon the initial vibrational state of the molecule and therefore shows a trend that is more similar to that seen by the experiments on vibrational deexcitation. We can therefore surmise that such an independence of the initial vibrational state for the relaxation rate shown by real systems can be partly related to the higher density of vibrational states exhibited by the heavier diatomic molecules involved in those processes.

ACKNOWLEDGMENTS

We thank the CASPUR Supercomputing Consortium for its computational help, the University of Rome "La Sapienza" Research Committee, and the "Cold Molecules Network" Grant No. HPRN-CT-2002-00290. We are also grateful to Professor M. Weidemueller for informing us of his results prior to their publication.

[1] H. L. Bethlem and G. Meijer, Int. Rev. Phys. Chem. **22**, 73 (2003).
[2] J. Doyle, B. Friedrich, R. V. Krems, and F. Masnou-Seeuws, Eur. Phys. J. D **31**, 149 (2004).
[3] R. V. Krems, Int. Rev. Phys. Chem. **24**, 99 (2005).
[4] R. Grimm, Nature (London) **435**, 1035 (2005).
[5] C. M. Dion, C. Drag, O. Dulieu, B. Labwrthe-Tolra, F. Masnou-Seeuws, and P. Pillet, Phys. Rev. Lett. **86**, 2253 (2001).
[6] S. Jochim, M. Bartenstein, A. Altmeyer, G. Hendl, S. Riedl, C. Chin, J. D. Denshlag, and R. Grimm, Science **302**, 2101 (2003).
[7] M. W. Zwierlein, C. A. Stan, C. H. Schunck, S. M. F. Raupach, S. Gupta, Z. Hadzibabic, and W. Ketterle, Phys. Rev. Lett. **91**, 250401 (2003).
[8] T. Mukaiyama, J. R. Abo-Shaeer, K. Xu, J. K. Chin, and W. Ketterle, Phys. Rev. Lett. **92**, 180402 (2004).
[9] C. Chin, T. Kraemer, M. Mark, J. Herbig, P. Waldburger, H.-C. Nägerl, and R. Grimm, Phys. Rev. Lett. **94**, 123201 (2005).
[10] D. S. Petrov, Phys. Rev. A **67**, 010703(R) (2003).
[11] D. S. Petrov, C. Salomon, and G. V. Shlyapnikov, Phys. Rev. Lett. **93**, 090404 (2004).
[12] D. S. Petrov, C. Salomon, and G. V. Shlyapnikov, Phys. Rev. A **71**, 012708 (2005).
[13] J. M. Doyle, B. Friedrich, J. Kim, and D. Patterson, Phys. Rev. A **52**, R2515 (1995).
[14] J. Weinstein, R. deCarvalho, T. Guillet, B. Friedrich, and J. M. Doyle, Nature (London) **395**, 148 (1998).
[15] N. Balakrishnan, G. C. Groenenboom, R. V. Krems, and A. Dalgarno, J. Chem. Phys. **118**, 7386 (2003).
[16] R. C. Forrey, Eur. Phys. J. D **31**, 409 (2004).
[17] N. Balakrishnan, R. Forrey, and A. Dalgarno, Chem. Phys. Lett. **280**, 1 (1997).
[18] N. Balakrishnan, V. Kharchenko, R. C. Forrey, and A. Dalgarno, Chem. Phys. Lett. **280**, 5 (1997).
[19] N. Balakrishnan, R. C. Forrey, and A. Dalgarno, Phys. Rev. Lett. **80**, 3224 (1998).
[20] E. Bodo and F. A. Gianturco, J. Phys. Chem. A **107**, 7328 (2003).
[21] T. Stoecklin, A. Voronin, and J. C. Rayez, Phys. Rev. A **66**,

042703 (2002).
[22] T. Stoecklin, A. Voronin, and J. C. Rayez, Phys. Rev. A **68**, 032716 (2003).
[23] M. T. Cvitaš, P. Soldán, J. M. Hutson, P. Honvault, and J.-M. Launay, Phys. Rev. Lett. **94**, 033201 (2005).
[24] G. Quéméner, P. Honvault, J.-M. Launay, P. Soldán, D. E. Potter, and J. M. Hutson, Phys. Rev. A **71**, 032722 (2005).
[25] P. Staanum, S. D. Kraft, J. Lange, R. Wester, and M. Weidemüller, Phys. Rev. Lett. **96**, 023201 (2006).
[26] N. Zahzam, T. Vogt, M. Mudrich, D. Comparat, and P. Pillet, Phys. Rev. Lett. **96**, 023202 (2006).
[27] P. E. Wigner, Phys. Rev. **73**, 1002 (1948).
[28] F. A. Gianturco, S. Serna, G. Delgado-Barrio, and P. Villareal, J. Chem. Phys. **95**, 5024 (1991).
[29] E. Bodo, F. Sebastianelli, F. A. Gianturco, E. Yurtsever, and M. Yurtsever, J. Chem. Phys. **120**, 9160 (2004).
[30] E. Bodo, F. A. Gianturco, and E. Yurtsever, J. Low Temp. Phys. **138**, 259 (2005).
[31] A. Aguado, C. Tablero, and M. Paniagua, Comput. Phys. Commun. **108**, 259 (1998).
[32] K. T. T. U. Kleinekathofer, J. P. Toennies, and C. L. Yiu, Chem. Phys. Lett. **249**, 257 (1996).
[33] B. Barakat, R. Bacis, E. Carrot, S. Churrassy, P. Crozet, and F. Martin, Chem. Phys. **102**, 215 (1986).
[34] R. Cote, A. Dalgarno, and M. J. Jamieson, Phys. Rev. A **50**, 399 (1994).
[35] B. C. Garrett, G. C. Lynch, T. C. Allison, and D. G. Truhlar, Comput. Phys. Commun. **109**, 47 (1998).
[36] P. Siegbahn and B. Liu, J. Chem. Phys. **68**, 2457 (1978).
[37] D. G. Truhlar and C. J. Horowitz, J. Chem. Phys. **68**, 2466 (1978).
[38] D. G. Truhlar and C. J. Horowitz, J. Chem. Phys. **71**, 1514 (1979).